Macromolecules

ARTICLE

pubs.acs.org/Macromolecules

Synthesis of Well-Defined (Nitrilotriacetic Acid)-End-Functionalized Polystyrenes and Their Bioconjugation with Histidine-Tagged Green Fluorescent Proteins

Hong Y. Cho,[†] Mohammad Abdul Kadir,[†] Bong-Soo Kim,[†] Ho Seok Han,[†] Soundrarajan Nagasundarapandian,[‡] Young-Rok Kim,[§] Sung Bo Ko,[⊥] Sun-Gu Lee,[‡] and Hyun-jong Paik*[,†]

[†]Department of Polymer Science & Engineering, Pusan National University, Busan 609-735, Korea

[‡]Department of Chemical Engineering, Pusan National University, San 30 Jangjeon 2-dong Geumjeong-gu, Busan 609-735, Korea

[§]Department of Food Science and Biotechnology & Institute of Life Sciences and Resources, College of Life Sciences, Kyung Hee University, Yongin, Korea

[⊥]MediGen Inc., 461-6 Jeonmin-Dong, Yuseong-Gu, Daejon 305-811, Korea

Supporting Information

ABSTRACT: We have synthesized nitrilotriacetic acid end-functionalized polystyrene (NTA−PS) for the controlled bioconjugation with histidine-tagged green fluorescence proteins (His_6−GFP). NTA−PS was prepared using initiators containing *tert*-butyl protected NTA moiety via atom transfer radical polymerization (ATRP) of styrene; the protected *tert*-butyl group was subsequently removed at the α-chain end of polystyrene. The structure of NTA−PS was characterized using ^1H NMR, ^{13}C NMR, and GPC. NTA chain ends of the polystyrenes were complexed with Ni^{2+} to produce Ni−NTA−PS, of which the specific binding properties were studied by forming spherical aggregates with His_6−GFP in aqueous phase. The reversible association of His_6−GFP with polystyrene spherical aggregates (with Ni^{2+}) was controlled with imidazole and monitored with fluorescence microscope. Again, Ni−NTA−PS produced well-defined micelles with His_6−GFP in water/DMF (DMF 4 vol %) and the size of micelles decreased when excess imidazole was added.

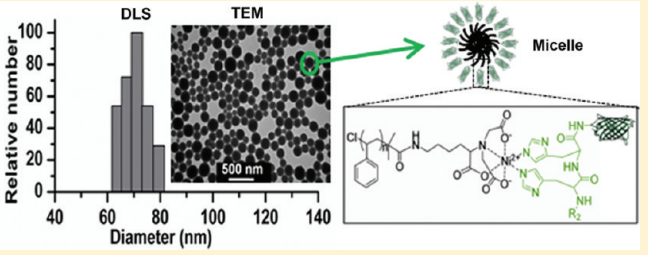

INTRODUCTION

Polymers with chain ends attached to proteins have potential applications in pharmaceuticals and biotechnology,[1−5] as they can effectively improve protein stability, solubility, and biocompatibility.[6,7] The plausible applications include protein delivery,[8,9] enzyme immobilization,[10] and biosensors.[11−13] Recently, conjugates between natural proteins and synthetic polymers have been receiving increasing research interests in material science areas with expectations of providing new routes for preparation of biologically functional structures[14−17] by synergistic action from two distinctive materials.[18] In addition, synthetic polymers attached to proteins impart new properties such as self-assembly and phase behavior.

Although applications of bioconjugates of proteins are being introduced, the reliable and efficient methodologies of producing stable bioconjugates in a controlled fashion are still challenging. In this respect, well-defined polymers have been explored to combine with proteins of specific reactivity. Recent advances in polymer synthesis, in particular, controlled radical polymerizations (CRPs), provided avenues to polymers with well-defined composition, molecular shape, chain length, and α,ω-functionality.[19] The reactive chain-ends could be used to conjugate some functional proteins. For example, using CRPs,[20] well-defined polymers with *N*-succinimide ester,[21,22] aldehyde,[23] thiol, maleimide,[24,25] or pyridyl disulfide[26] chain-ends have been used to conjugate with targeted proteins.

While majorities of polymer and protein studies focused on covalent bioconjugation, only limited studies were reported on noncovalent approaches.[27,28] Some representative examples include avidin/streptavidin−biotin couples,[29−31] sugar−protein interactions,[32] and heme-modified cofactor−protein.[33] Since both Avidin (Av) and streptavidin (SAv) have very strong affinity toward biotin,[34,35] well-defined poly(*N*-isopropylacrylamide) with biotin chain-end was shown to bind to SAv.[29] The conjugation was accomplished using biotinylated chain end introduced via ATRP initiator and confirmed by SDS-PAGE.[30] In another example, a SAv tetra-functionalized ATRP initiator was used to polymerize *N*-isopropylacrylamide (NIPAM) by atom transfer radical polymerization (ATRP) in water.[31] Also, ATRP and "*click*" chemistry were combined to prepare sugar-protein conjugate.[32]

An alternative noncovalent approach would be to use polymers containing Ni^{2+} complexed nitrilotriacetic acid (Ni−NTA) for

Received: March 1, 2011
Revised: May 17, 2011
Published: June 06, 2011

Scheme 1. Preparation of Ni^{2+}-Complexed-NTA End-Functionalized Polystyrene (Ni−NTA−PS)

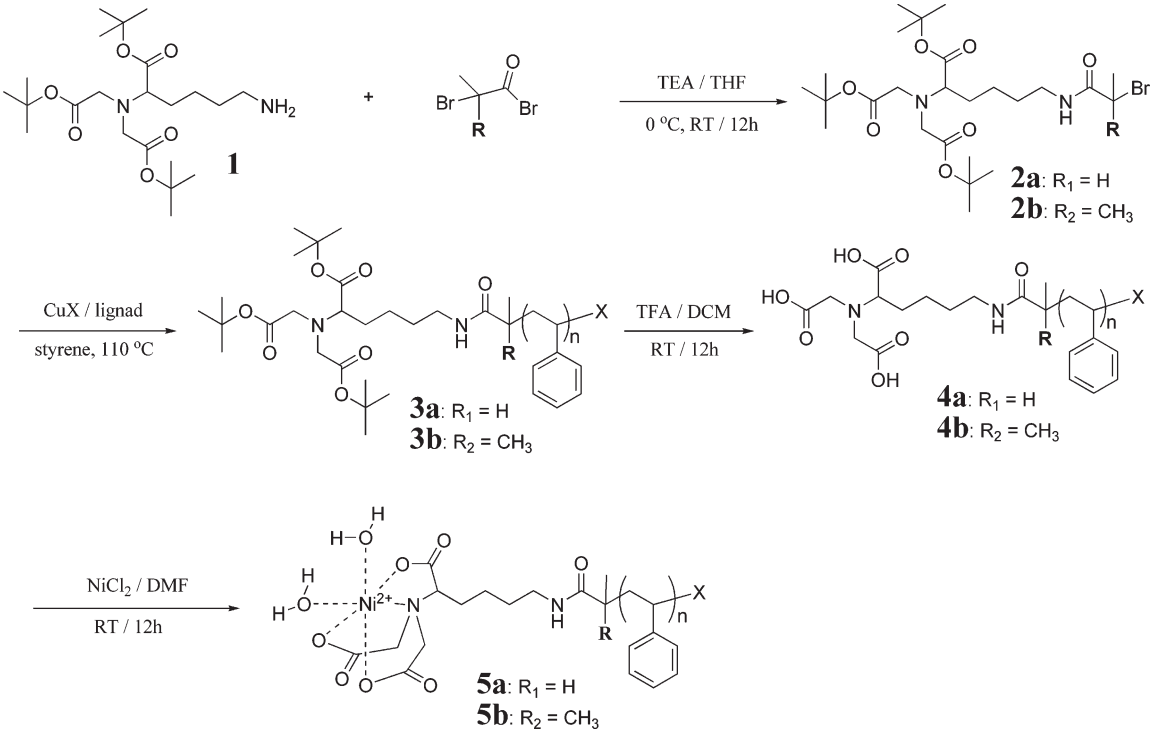

bioconjugation with genetically modified Histidine-tagged (His-tag) proteins. His-tags bound to either the C- or N-terminus are commercially available for a large number of proteins/enzymes. Therefore, it could be a general approach for a large number of proteins/enzymes. NTA is a tetradentate ligand which occupies four of the six binding sites of Ni^{2+}, leaving two free sites for His-tag proteins to bind. The NTA chelating chemistry with His-tag proteins offers several advantages of biochemical recognition elements. First, the Ni^{2+} complexation with a histidine is fast and reversible reaction, where competitor ligand, such as imidazole could displace the His-tag proteins. Second, Ni^{2+}−NTA complexation is a very well established and efficient immobilization system in biology. Transition metals chelated by NTA or other chelators were successfully applied for the purification[36−39] and detection[36,40] of oligohistidine-tagged proteins, as well as for surface immobilizations[41−45] and for tethering to lipid membranes.[46−48]

For conjugation of protein with polymers, Kiessling et al. synthesized poly(*N*-methacryloxysuccinimide) using ATRP, where NTA derivatives were appended to the polymer backbone. After nickel complexation, His-tagged fibroblast growth factor 8b (His-tag FGF-8b) was clustered with NTA moiety through noncovalent interaction.[49] Ober et al. polymerized acrylamide monomer with an NTA moiety, which was incorporated into 2-hydroxyethyl methacrylate (HEMA) hydrogels in a controlled fashion for the specific protein immobilization.[50] Similar studies were reported by Kopecek et al. using iminodiacetate (IDA)−Ni^{2+} and His-tag protein. They utilized nickel IDA complex for poly(HPMA-*co*-DAMA) hybrid hydrogel primary chains and for the attachment of His-tag coiled-coil proteins.[51]

In this report, we describe the synthesis of NTA end-functionalized polystyrenes by ATRP and their use for bioconjugation with His_6−GFP to produce self-assembled structures in aqueous system. Therefore, we synthesized NTA end-functionalized polystyrene, **4b**, by ATRP in a controlled fashion. As shown in Scheme 1, we prepared alkyl halide with protected NTA moieties, **2**, and used them for the initiation of styrene ATRP, followed by removal of protecting *tert*-butyl groups. In the aqueous system, polystyrene spherical aggregates, as in **4b** (with NTA end group) and **5b** (with Ni−NTA end group), were generated through solvent evaporation method. Similar studies were carried out by Nolte et al. that demonstrated the aggregation behavior of heme-modified PS,[33] which were comparable to the micelles of amphiphilic block copolymers.[52] The reversible association of His_6−GFP with polystyrene spherical aggregates (with Ni^{2+}) was controlled with excess imidazole and monitored with fluorescence microscope. Again, Ni−NTA−PS (M_n = 21 800) produced well-defined micelles with His_6−GFP in water/DMF (DMF 4 vol %) and the size of micelles decreased when excess imidazole was added.

EXPERIMENTAL SECTION

Materials. Styrene (Junsei, 99.5%) was purified by vacuum distillation over CaH_2. Cu(I)Br (Aldrich, 98%) and Cu(I)Cl (Aldrich, 98%) were purified by stirring with glacial acetic acid followed by filtering and washing the resulting solids with ethanol (× 3) and diethyl ether (× 2), respectively. *N*,*N*,*N*′,*N*′′,*N*′′-penetamethyldiethylenetriamine (PMDETA) (Aldrich, 98%) was purified by vacuum distillation. 4,4′-di(5-nonyl)-2,2′-bipyridine (dNbpy) (97%), *tert*-butyl bromoacetate (98%), 2,2′-dipyridyl (bpy) (99%+), palladium (10 wt % activated carbon), 2-bromoisobutyryl bromide (98%), and 2-bromopropionyl bromide (97%) were purchased from Aldrich and used as received. *H*-Lysine(*Z*)−OtBu·HCl was used as received (Bachem, 99%+). *N*,*N*-bis[(*tert*-butyloxycarbonyl)methyl]-L-lysine *tert*-butyl ester (**1**) was synthesized by following the reported procedure.[53]

Measurements. Molecular weight (M_n) and molecular weight distribution (M_w/M_n) were determined using gel permeation

Table 1. ATRP of Styrene Using NTA Derivative Initiators at 110 °C[a]

no.	$[M]_0/[I]_0$	$[I]_0$	catalyst	time [h]	convn [%]	$M_{n,GPC}$ [10^3]	M_w/M_n	$M_{n,theory}$[b] [10^3]
1	672	**2a**	CuBr/PMDETA	17	34	154	1.45	24.7
2	672	**2a**	CuCl/PMDETA	7	26	170	1.67	18.7
3	196	**2a**	CuCl/2dNbpy	5.75	27	11.0	1.26	6.1
4	196	**2b**	CuCl/2dNbpy	14	55	13.5	1.21	11.8
5	48	**2b**	CuCl/2dNbpy	14	72	4.9	1.09	4.2
6	29	**2b**	CuCl/2dNbpy	20	70	3.9	1.08	2.7

[a] 1: $[\text{styrene}]_0$ = 7.9 M, $[\text{initiator}]_0 = [\text{CuBr/PMDETA}]_0 = 1.2 \times 10^{-2}$ M, anisole =7.8 × 10^{-1} mL. 2: $[\text{styrene}]_0$ = 4.3 M, $2[\text{initiator}]_0 = [\text{CuCl/PMDETA}]_0 = 1.3 \times 10^{-2}$ M, anisole =7.8 mL. 3: $[\text{styrene}]_0$ = 4.3 M, $2[\text{initiator}]_0 = [\text{CuCl/2dNbpy}]_0 = 4.5 \times 10^{-2}$ M, anisole =1.5 mL. 4: $[\text{styrene}]_0$ = 4.3 M, $2[\text{initiator}]_0 = [\text{CuCl/2dNbpy}]_0 = 4.5 \times 10^{-2}$ M, anisole =1.5 mL. 5: $[\text{styrene}]_0$ = 4.3 M, $2[\text{initiator}]_0 = [\text{CuCl/2dNbpy}]_0 = 1.8 \times 10^{-1}$ M, anisole =1.0 mL. 6: $[\text{styrene}]_0$ = 4.3 M, $[\text{initiator}]_0 = [\text{CuCl/2dNbpy}]_0 = 1.5 \times 10^{-1}$ M, anisole = 3.0 mL. [b] $M_{n,theory}$ = conversion × $([\text{monomer}]_0/[\text{initiator}]_0) \times M_{monomer} + M_{initiator}$

chromatography (GPC), which was precalibrated with polystyrene standards. GPC was equipped with Agilent 1100 pump, RID detector, and PSS SDV (5 μm, 10^5, 10^3, 10^2 Å 8.0 × 300.0 mm) columns. Monomer conversion was determined by HP 5890 gas chromatography, equipped with HP101 column (methyl silicone fluid, 25 m × 0.32 mm ×0.3 μm). ^{1}H and ^{13}C NMR spectra were obtained using Varian Unity Plus 300 or Inova 500 FT-NMR spectrometers. Transmission electron microscope (TEM) and scanning electron microscope (SEM) images were obtained on a Hitachi H-7600 instrument at 100 kV and on a Hitachi S-4200, respectively. Energy Dispersive X-ray fluorescence analysis (EDX, Horiba/EX-250) results were obtained by Hitachi/E-1030 ion sputter with Nikon/SMZ-U stereomicroscope. For microscopic analysis, TEM samples were prepared by dipping a TEM grid (carbon coated grid) into respective solutions. SEM/EDX samples were prepared by dropping solution onto the silicon wafer. Extra solution was blotted with filter paper and dried for 12 h at room temperature. Differential scanning calorimeter (DSC) analyses were performed with TA Instruments Q100, which operated at a 10 °C/min under nitrogen gas. Fluorescence optical microscope images were obtained on Nikon TE2000-U. Dynamic light scattering (DLS) studies were performed with 90 Plus, Particle Size Analyzer, Brookhaven Instruments Corporation. The photoluminescence (PL) spectra were recorded using an Ocean Optics HR4000CG Composite-grating spectrophotometer with an excitation wavelength at 395 nm.

Synthesis of *N,N*-Bis[(*tert*-butyloxycarbonyl)methyl]-*N′*-2-bromopropionyl-L-lysine *tert*-Butyl Ester (2a). Under nitrogen, 2-bromopropionyl bromide (90.0 μL, 8.5 × 10^{-1} mmol) was added dropwise to a stirring mixture of **1** (342 mg, 7.7 × 10^{-1} mmol) and triethylamine (320 μL, 2.3 mmol) in 50.0 mL THF in an ice bath for 1 h. Upon complete addition of the acid bromide, the mixture was stirred at room temperature for 12 h. After evaporation of THF, the mixture was dissolved in 100 mL of CH_2Cl_2 and washed with water (5 × 100 mL). The crude product was purified by column chromatography, eluting with 4:1 *n*-hexane/ethyl acetate: yielding sample with the following NMR analysis. ^{1}H NMR (300 MHz, $CDCl_3$): δ 1.38 (s, 18H), 1.40 (s, 9H), 1.49 (m, 2H), 1.60 (m, 2H), 1.65 (m, 2H), 1.88 (s, 3H) 3.20 (t, 2H), 3.25 (t, 1H), 3.42 (dd, 4H), 4.41 (q, 1H). MS (ESI−MASS): found, 589 ($M + Na^+$); *m/z* calculated for $C_{25}H_{45}N_2O_7Br_1Na_1$, 589.

Synthesis of *N,N*-Bis[(*tert*-butyloxycarbonyl)methyl]-*N′*-2-bromoisobutyryl-L-lysine *tert*-Butyl Ester (2b). **2b** was prepared in a procedure similar to that used for **2a**, where 2-bromoisobutyryl bromide was used, instead of 2-bromopropionyl bromide, yielding a sample with the following NMR analysis. ^{1}H NMR (300 MHz, $CDCl_3$): δ 1.38(s, 18H), 1.40 (s, 9H), 1.49 (m, 2H), 1.60 (m, 2H), 1.65 (m, 2H), 1.88 (s, 6H) 3.20 (t, 2H), 3.25 (t, 1H), 3.42 (dd, 4H); MS (ESI−MASS): found, 601 ($M + Na^+$); *m/z* calculated for $C_{26}H_{47}N_2O_7Br_1Na_1$, 601.

Synthesis of Polystyrene 3b. Styrene (1.00 mL, 8.82 mmol) and anisole (1.00 mL) were added to a N_2-purged Schlenk flask. After three freeze−pump−thaw cycles, Cu^ICl (36.4 mg, 0.368 mmol) and dNbpy (300.8 mg, 0.736 mmol) were added to the flask, followed by two freeze−pump−thaw cycles. The flask was placed into an oil bath set at 110 °C. Then initiator **2b** (106.5 mg, 0.184 mmol) was added to the flask. At timed intervals, aliquots of 0.05 mL of the reaction mixture were taken and diluted in THF for GC and GPC analysis. The product was precipitated against MeOH and dried *in vacuo* at 45 °C for 12 h.

Deprotection of *tert*-butyl group in 3b. Polystyrene **3b** (300 mg, 61.2 × 10^{-3} mmol) and trifluoroacetic acid (TFA, 136.4 μL, 18.6 × 10^{-1} mmol) were stirred in 20.0 mL of CH_2Cl_2 at room temperature for 12 h. The solvent was evaporated under reduced pressure. The resulting product was purified by precipitation against MeOH and dried *in vacuo* at 45 °C for 12 h.

Nickel Complexation of 4b. Polystyrene **4b** (100 mg, 21.3 × 10^{-3} mmol) was dissolved in 50 mL of DMF in the flask, followed by addition of nickel chloride ($NiCl_2$, 54.4 mg, 0.420 mmol). The complexation was carried out by stirring at room temperature for 12 h. The mixture was purified by precipitation against MeOH and then dried *in vacuo* at 45 °C for 12 h.

Preparation of Aggregates of 4b and 5b. H_2O (8 mL) was slowly added to 2 mg of **4b** and **5b** in THF (2 mL), under rapid stirring. The mixture was continually stirred for 3 h at 60 °C. After complete removal of THF, the resulting aqueous solution was sonicated for 30 min and kept at −4 °C.

Expression and Purification of His_6−GFP. *Escherichia coli* BL21 (DE3) harboring the pET−GFPmut3.1 expressing GFPmut3.1[54] tagged with hexahistidine at its N-terminus was grown to OD600 of 0.6 at 37 °C in 100 mL of Luria−Bertani (LB) medium containing 100 μg/mL of ampicillin, induced with 0.05 mM isopropyl β-D-thiogalactopyranoside (IPTG) for 6 h at 37 °C, and pelleted. Cells were lysed by using BugBuster protein extraction kit (Novagen). Briefly, collected cell pellet was resuspended in 5 mL of lysis buffer, incubated at room temperature for 10 min, and centrifuged for 20 min at 9,000 g and 4 °C. After the extracts was incubated with 5 mg of Ni−NTA HisBind Resin (Novagen) for 3 h at 4 °C, the resin was loaded into column, washed with 2 × 4 mL of washing buffer (50 mM phosphate buffer, pH 8.0; 300 mM NaCl; 20 mM imidazole), and the His_6−GFP was eluted with 1 mL of elution buffer (50 mM phosphate buffer, pH 8.0; 300 mM NaCl; 250 mM imidazole). Imidazole in the eluted solution was removed by Diafiltration (Millipore). The protein fractions were analyzed by SDS-PAGE (12% acrylamide gel), showing that the purity of purified His_6−GFP was more than 95%.

Conjugation of His_6−GFP with 4b and 5b. Aggregate solution (300 μL) was spun down at 10 000*g* for 3 min. After discarding the supernatant, the pellet was resuspended in 500 μL PBS with 1% BSA (w/v) and incubated for 10 min in rotating rack. Washing step was repeated three times. After the final wash, 3 μL His_6−GFP solution were added with the pellet and incubated for 10 min in rotating rack. The pellet was spun down at 10 000*g* for 3 min and washed with 200 μL of

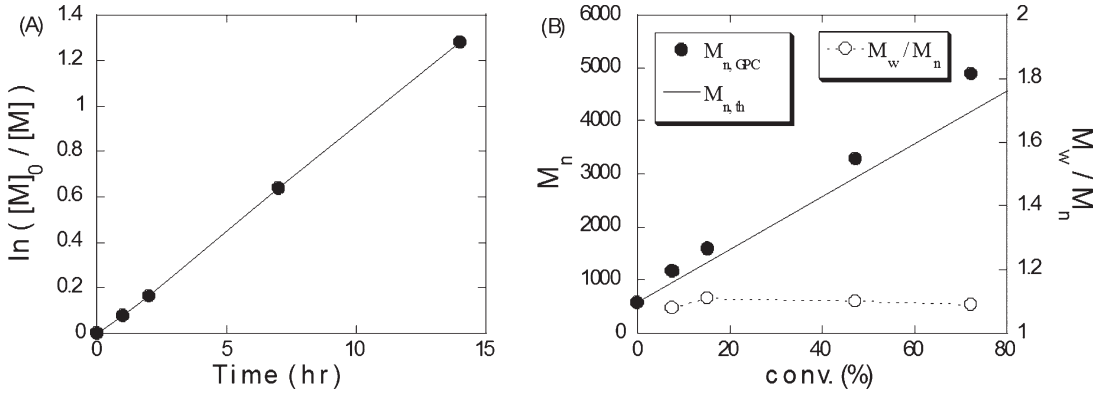

Figure 1. Results of styrene ATRP using **2b** (entry 5, Table 1): (A) first-order kinetic plots; (B) M_n and M_w/M_n evolution on monomer conversion.

PBS with 1% BSA (w/v), and 2 μL of pellets were examined with fluorescence microscope.

Release of His_6—GFP with Imidazole. 300 μL imidazole solution (250 mM) was added to 300 μL of conjugated aggregate solution with His_6—GFP, followed by sonication for 10 min. The solution was spun down at 10 000*g* for 10 min. After removing supernatant, the pellet was resuspended in 200 μL of PBS with 1% BSA (w/v), and 20 μL of the pellets were examined with fluorescence microscope.

RESULTS AND DISCUSSION

Synthesis. Initiators, containing the activated alkyl bromide, were prepared to introduce NTA functional group at α-chain end of polymers using ATRP. In order to ensure high solubility of the initiator and prevent side reactions (protonation of ATRP ligand), *tert*-butyl protected NTA-based amidic initiators[55,56] were designed (**2a** or **2b**). Initially, **2a** was prepared by the amidation reaction of protected aminobutyl NTA with 2-bromopropionyl bromide (Scheme 1). The polymerization of styrene was carried out with **2a** using CuBr/PMDETA, which is the frequently used ATRP catalytic system (entry 1 in Table 1).[57] However, the resulting polymers displayed higher molecular weights than expected and showed broad molecular weight distribution (MWD) at low conversion. This result indicated that the initiation of styrene ATRP by **2a** was slow, as reported previously in literature.[58,59]

In order to improve initiation efficiency, a technique known as halogen exchange was employed.[60] In the halogen exchange, CuCl catalyst was used with the alkyl bromide initiator. Hence, NTA—PS was synthesized with **2a** using CuCl/PMDETA instead of CuBr/PMDETA. However, the results of polymerization showed again a typical slow initiation behavior, yielding polymers with higher molecular weight and broad MWD (entry 2 in Table 1). These results showed that halogen exchange method was not effective in the polymerization of styrene with the propionamide-based alkyl bromide initiator (**2a**) and CuCl/PMDETA catalyst. When the ligand for catalyst was changed from PMDETA to a bipyridine-based ligand, dNbpy, the polymerization of styrene showed better control (entry 3 in Table 1). The polymerization with initiator **2b** together with dNbpy yielded well-controlled polystyrene, **5** (entries 4—6 in Table 1) as **2b** initiator showed fast activation rate. In addition, fast deactivation rate with bpy based catalyst may also contribute to the improvement of initiation efficiency.[61]

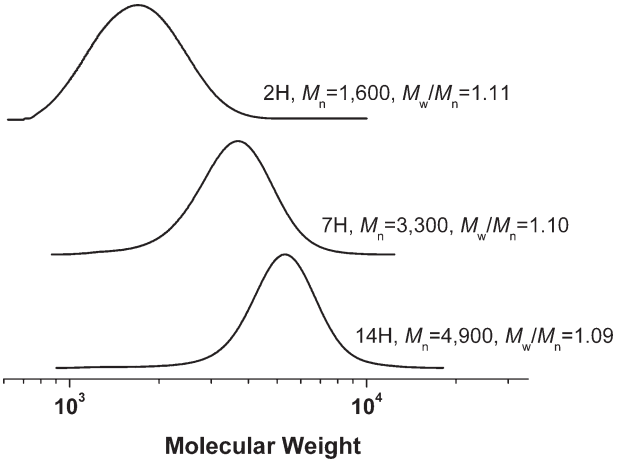

Figure 2. Gel permeation chromatogram traces of NTA—PS (entry 5, Table 1).

The polymerization of styrene with **2b** and CuCl/dNbpy showed typical characteristics of living polymerization. The first order kinetic plot was linear and the rate of radical generation was faster than that of **2a**. The molecular weight increased linearly with conversion, which showed good agreement with theoretical molecular weight. The molecular weight distribution was narrow as 1.09 (Figure 1 and Figure 2).

Presence of NTA moiety in PS (entry 6 in Table 1) was verified by ^{1}H NMR and ^{13}C NMR (Figure 3 and 4). Peaks at 1.33 (a, $(CH_3)_3$—) and 1.35 ppm (b, $(CH_3)_3$—) were assigned to *tert*-butyl protons and peaks at 2.71 (h, —CH_2—), 3.15 (d, —CH—), 3.38 (c, —CH_2—) 4.25 (n, —CH—Cl) and 5.17 (i, —NH—) ppm were clearly assigned to NTA moiety in Figure 3A, which indicated that **2b** was successfully used as ATRP initiator. Based on the integral ratio of peak h (2.6—2.8 ppm), to the phenyl ring proton (6.2—7.4 ppm), the M_n of **3b** was calculated to be 4500 g/mol. M_n calculated from ^{1}H NMR agreed well with those from GPC ($M_{n,GPC}$ = 3900).

NTA-end-functionalized polystyrene, **4b** was obtained by removing *tert*-butyl groups of **3b** with TFA in CH_2Cl_2. The structure of **4b** was confirmed by ^{1}H and ^{13}C NMR. Mixed solvent of $CDCl_3$/MeOD-d_4 = 99/1 by vol % was used for ^{1}H NMR. After the deprotection, hydrophilic nature of NTA chain-end of polystyrene would result in the restriction of the segmental motion and mobility of the polymer components in $CDCl_3$. This restriction of the motion of polymer molecular chains would have significant

dx.doi.org/10.1021/ma200480f |*Macromolecules* 2011, 44, 4672–4680

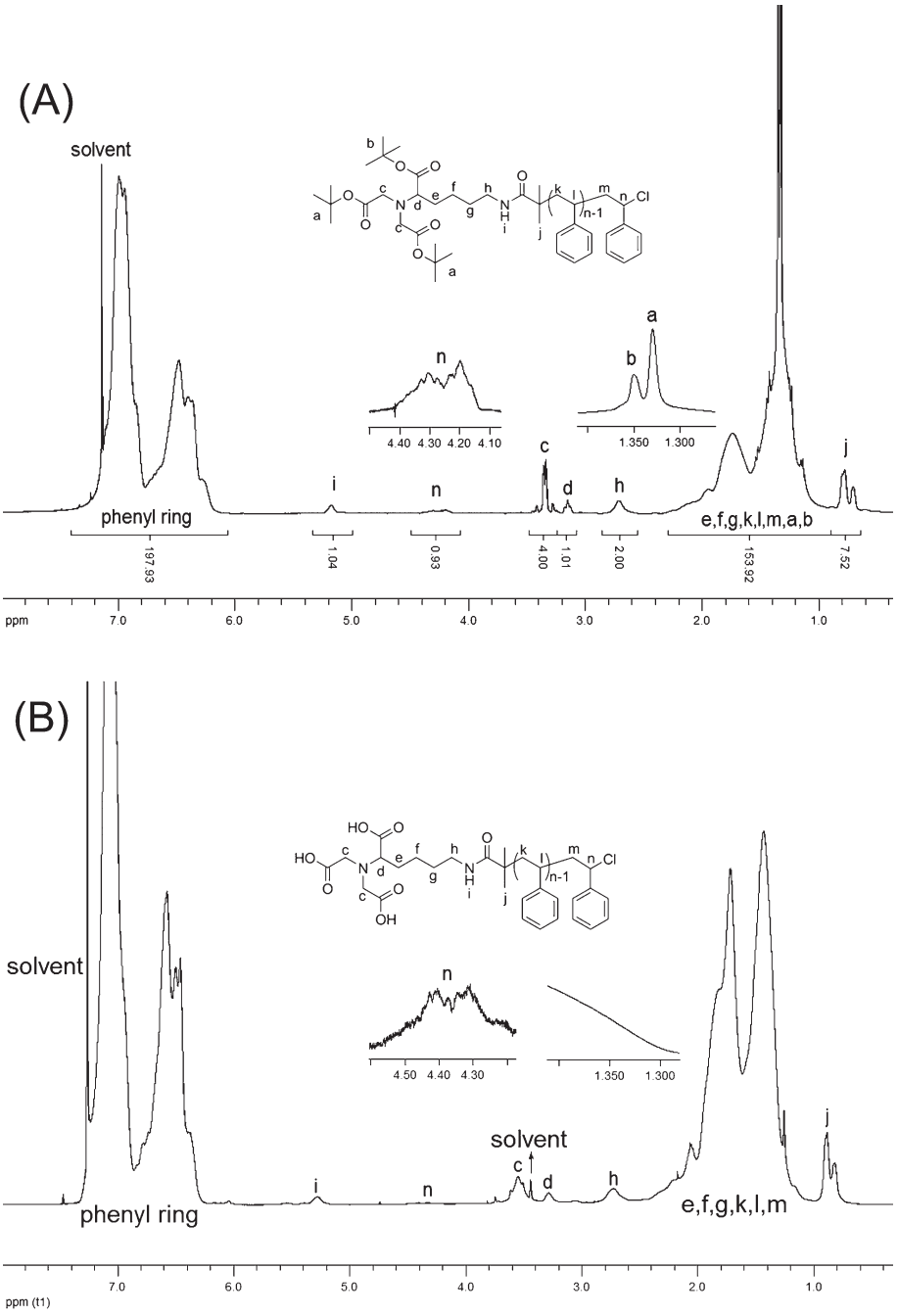

Figure 3. (A) ^{1}H NMR spectra of α-(*p*-NTA)−polystyrene, **3b**, ($M_{n,\,GPC}$ = 3900; M_w/M_n = 1.08,), $CDCl_3$ 100%, and (B) α-(NTA)−polystyrene, **4b**, ($M_{n,GPC}$ = 3500; M_w/M_n = 1.18), mixed solvent system ($CDCl_3$/MeOH-d_4 = 99/1 by vol %).

effects on the spin−lattice relaxation time of their protons. With the addition of MeOD-d_4 (1 vol %) to $CDCl_3$, peaks from **4b** were clearly assigned. The chain end structures of polystyrene before and after deprotection were also confirmed by ^{13}C NMR spectra in Figure 4.

Successful transformation of chain-end to NTA was also supported by GPC analysis. Figure 5 showed that after removal of *tert*-butyl protecting groups, the peak molecular weight of NTA−PS decreased slightly, while the formation of high molecular weight species and significant tailing were observed. These observations could be explained by the effect of carboxylic acid groups at the polystyrene chain end, inducing the molecular association of **4b** through hydrogen bonding and interactions of **4b** with stationary phase in GPC analysis.[62,63]

Glass transition temperatures, T_g, were measured by DSC to further confirm the successful deprotection of *tert*-butyl groups of **3b**, as shown in Figure 6. **3b** (M_n = 3900) exhibited T_g at 78.5 °C, which was similar to T_g of prepared polystyrene (M_n = 3100, polystyrene$_{ATRP}$) using ATRP with 1-phenylethyl bromide as an initiator. After the deprotection, T_g of **4b** increased to 93.8 °C, suggesting that the carboxylic acid groups in polystyrene chain end played a role in heightening T_g of **3b**.[64,65] Increased T_g of **4b** could be attributed to the self-association of carboxyl end groups, reducing the polystyrene chain end mobility.

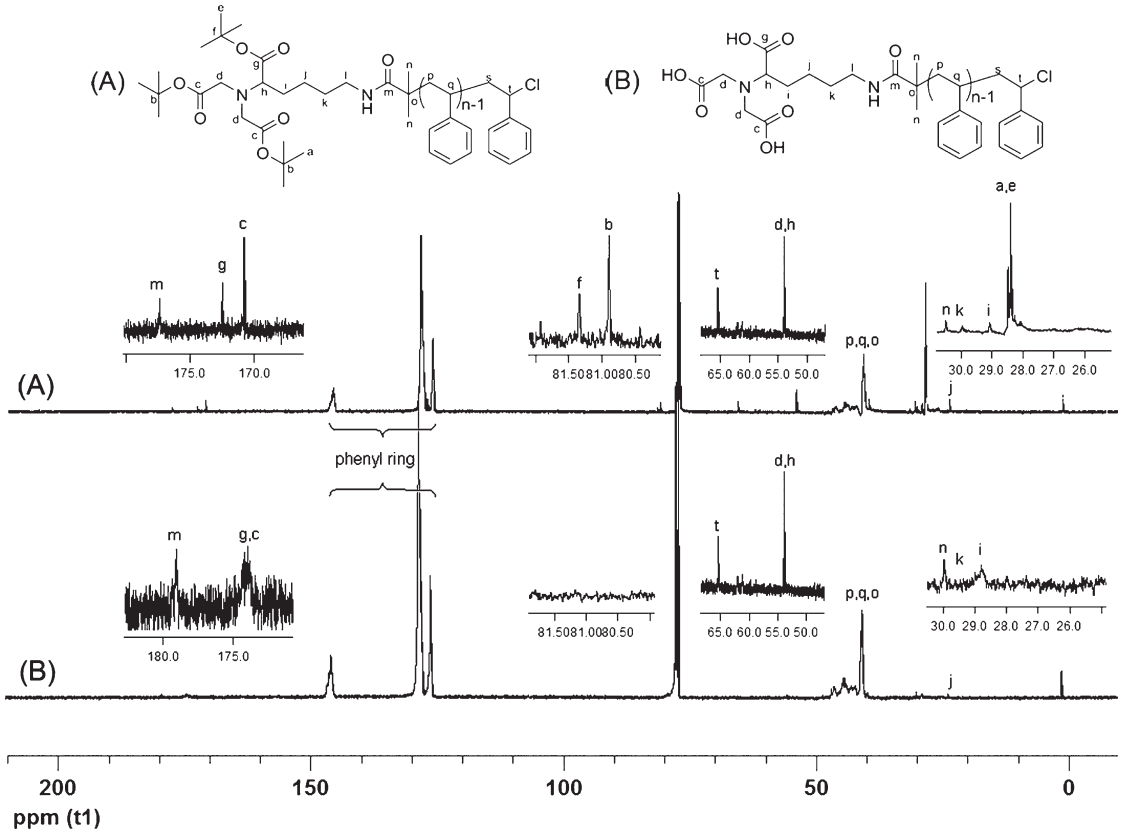

Figure 4. ^{13}C NMR spectra of p-NTA−PS, **3b**, ($M_{n,GPC}$ = 3900; M_w/M_n = 1.08), and NTA−PS, **4b**, ($M_{n,GPC}$ = 3500; M_w/M_n = 1.18).

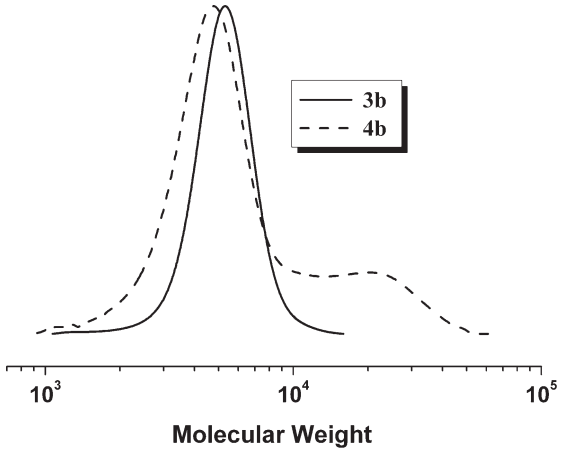

Figure 5. GPC chromatograms of α-(p-NTA)-polystyrene, **3b** ($M_{n,GPC}$ = 4900; M_w/M_n = 1.09) and α-NTA-polystyrene, **4b** ($M_{n,GPC}$ = 4700; M_w/M_n = 1.40).

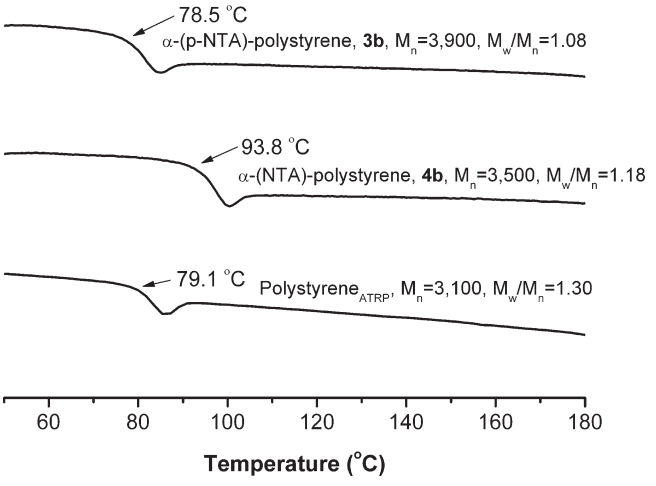

Figure 6. DSC curves of **3b**, **4b**, and polystyrene prepared using ATRP with 1-phenyl ethyl bromide as an initiator.

Conjugation of NTA End-Functionalized Polystyrene (NTA−PS) with His_6−GFP. The conjugation of NTA−PS with His_6−GFP and their self-assembly were studied by two different methods by changing solvent (THF and DMF) as well as molecular weight of the polymer (M_n = 4700 and M_n = 21 800) with water. In THF evaporation method, aggregates of **4b** (without Ni^{2+}) and **5b** (with Ni^{2+}) were prepared by the addition of water to THF solution containing **4b** and **5b**, respectively.[66] THF was evaporated by stirring the respective mixture at 60 °C. In both cases, SEM and TEM studies showed that the size of polymeric aggregates were nearly 500 nm without staining (Figure 7). Aggregates were spherical and relatively uniform in size. The presence of Ni^{2+} in the aggregates was confirmed by EDX analysis.

Fluorescence microscopy was used to compare the binding of His_6−GFP on the spherical aggregates produced from **4b** (without Ni^{2+}) and **5b** (with Ni^{2+}), respectively (Figure 8). His_6−GFP solution was added to spherical aggregate solution of **4b** and **5b**, respectively. The mixture was spun down and washed with PBS. The fluorescence intensity of **4b** (A-1) was weaker than

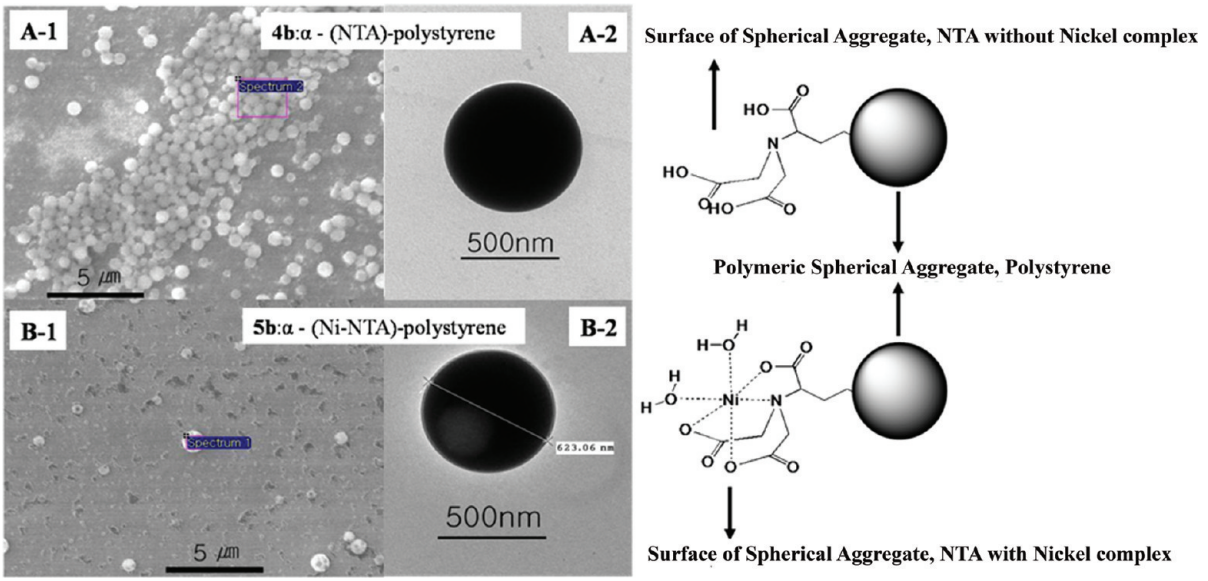

Figure 7. SEM and TEM images of the aggregates from the α-(NTA)-polystyrene. A-1 and A-2 are without nickel; B-1 and B-2 are with nickel.

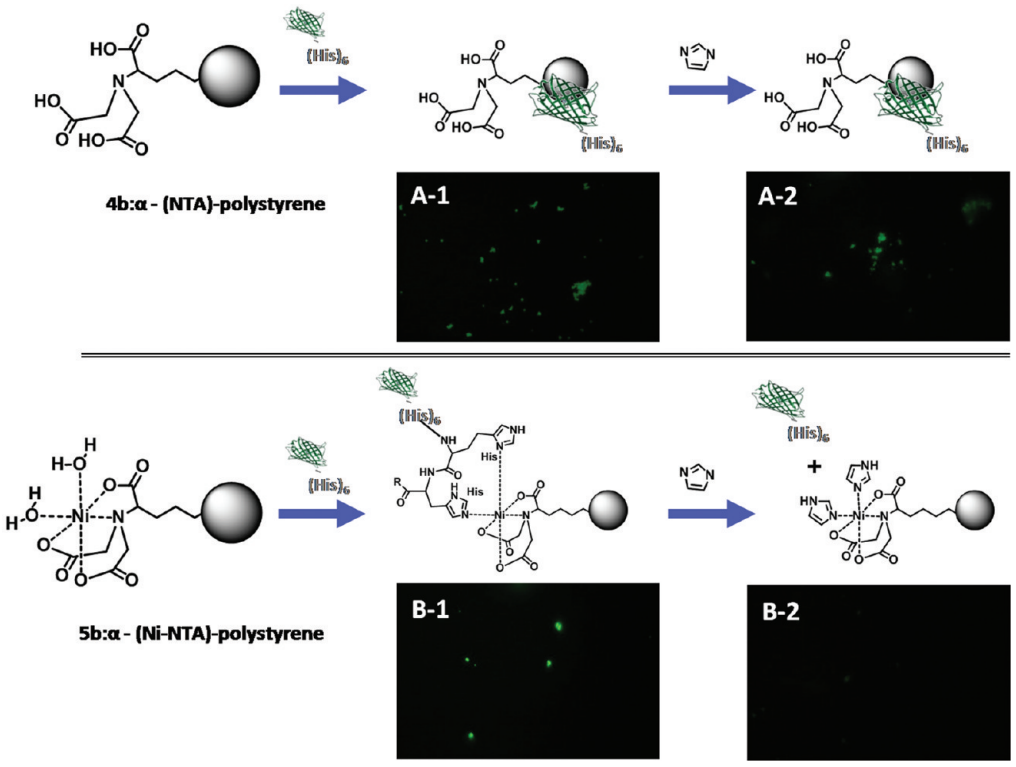

Figure 8. Fluorescence microscope images of the aggregates from the α-(NTA)-polystyrene: A-1, nonspecific binding of His_6−GFP with **4b**; A-2, binding after rinse with excess imidazole; B-1, specific binding of His_6−GFP to NTA of **5b** in presence of Ni; B-2, binding after rinse with excess imidazole.

that of **5b** (B-1), which could be due to the absence of nickel for chelating between His_6−GFP and NTA on the surface of spherical aggregates specifically (**4b**). According to Figure 8, adsorption of His_6−GFP on the surface of polystyrene spherical aggregates was irreversible and nonspecific, because the fluorescence intensity of **4b** did not decrease even after rinsing with excess of imidazole.

In the case of **5b**, the fluorescence intensity decreased from 100 (before rinsing with imidazole, Figure 8, B-1) to 14 (after rinsing with imidazole, Figure 8, B-2) due to the specific and reversible binding of nickel on the surface of **5b** with His_6−GFP.

To investigate self-assembled morphology of polymer−protein conjugate, we examined Ni−NTA−PS (M_n = 21,800) with water/DMF (See Supporting Information for bioconjugation

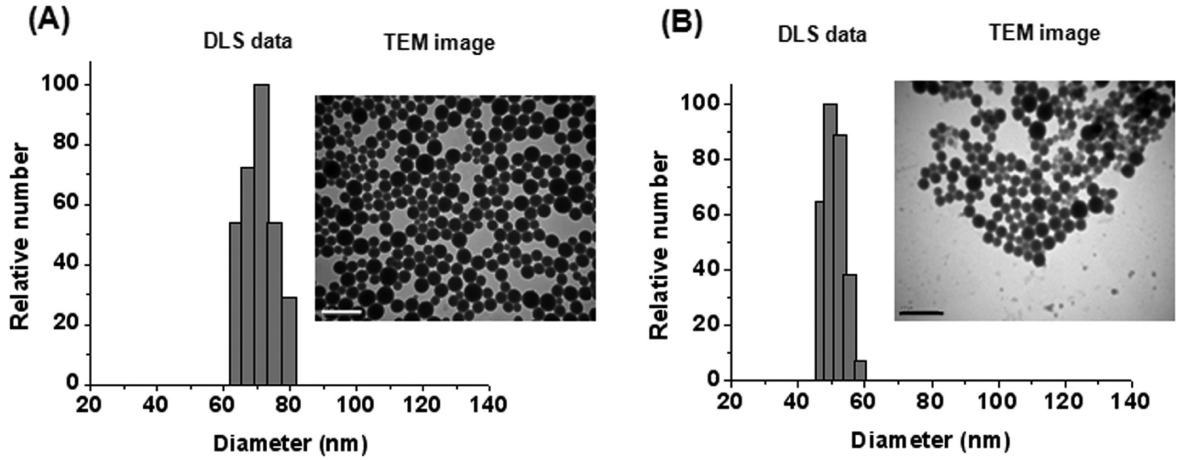

Figure 9. TEM and DLS data of Ni−NTA−PS (M_n = 21 800) with His_6−GFP in water/DMF: (A) after conjugation; (B) after addition of excess imidazole. Scale bar of TEM images = 500 nm.

experiment). Control experiment showed that the activity of GFP (fluorescence intensity) decreased with increasing the amount of DMF with water. Therefore, minimum amount of DMF (4 vol % of water) was added during conjugation experiment. The solution of Ni−NTA−PS in DMF was added slowly to deionized water using syringe pump with and without His_6−GFP under stirring. TEM and DLS studies showed that Ni−NTA−PS produced well-defined micelles with His_6−GFP (Figure 9A), while Ni−NTA−PS itself produced ill defined and larger aggregates without His_6−GFP (See Supporting Information, Figure SI-1).The reason of the former might be attributed to the amphiphilic nature of the polymer−protein conjugate due to specific interaction of polymer and protein via well established NTA−Ni^{2+}/His_6-tag interaction in water/DMF. To prove the binding of His_6−GFP with polymer via NTA−Ni^{2+}/His_6-tag interaction, a solution was filtered using centrifugal filter (Microcon, YM-100 membrane, NMWL-100 kDa). The fluorescence intensity of the initial solution, filtrate and retentate was measured by photoluminescence (PL) spectroscopy (See Supporting Information, Figure SI-2). The fluorescence intensity of the filtrate decreased compare to that of initial solution. This might be attributed to the presence of unbound GFP in filtrate, while most of the GFP remained as retentate due to specific binding with polymer during filtration process. The size of micelles decreased when competitor ligand (e.g.; imidazole) was added to the polymer−protein micellar solution. This might be due to the release of GFP by imidazole which was evidenced by TEM and DLS studies (Figure 9B).

CONCLUSIONS

In this study, the NTA chain-end functional groups in PS prepared by ATRP and the recombinant His_6−GFP were used to demonstrate the site specific and noncovalent bioconjugation between polymer and protein. First, alkyl halides with protected NTA moiety were synthesized and used as the initiators for ATRP of styrene. After removing the protecting *tert*-butyl groups, NTA end-functionalized PS with predetermined molecular weight and narrow molecular weight distribution was prepared. Through solvent evaporation method, spherical aggregates of α-(NTA)−polystyrene, **4b**, and α-(Ni−NTA)−polystyrene, **5b**, were yielded. Ni^{2+} chelation with NTA on the surface of polystyrene spherical aggregates was confirmed by SEM/EDX. Bioconjugation of His_6−GFP with **4b** and **5b** was investigated with florescence microscopy, revealing site-specific and reversible noncovalent bioconjugation between His_6−GFP and **5b**, whereas **4b** resulted in the nonspecific and irreversible binding. By means of imidazole treatment, the conjugation and release of His_6−GFP from α-(Ni−NTA)−polystyrene, **5b** were successfully controlled. Controlled bioconjugation of His-tagged protein with α-(Ni−NTA)−polystyrene may find broad applications in protein purification and enzyme immobilization.

ASSOCIATED CONTENT

Supporting Information. Bioconjugation experimental details in water/DMF, centrifuging procedure using membrane filter, TEM image (Figure SI-1), and photoluminescence (PL) spectra of polymer−protein conjugated solution, retentate and filtrate (Figure SI-2). This material is available free of charge via the Internet at http://pubs.acs.org.

AUTHOR INFORMATION

Corresponding Author

*Telephone: +82-51-510-2402. Fax: +82-51-513-7720. E-mail: hpaik@pusan.ac.kr.

ACKNOWLEDGMENT

The authors thank Professor Krzysztof Matyjaszewski (Department of Chemistry, Carnegie Mellon University) for valuable discussions. This work was supported by Basic Science Research Program (KRF-2007-331-D00130), the Active Polymer Center for Pattern Integration (R11-2007-050-02002-0) and WCU (World Class University) program (R33-10035-0) through the National Research Foundation (NRF) grant funded by the Korea government (MEST).

REFERENCES

(1) Duncan, R. *Nat. Rev. Drug Discov.* **2003**, *2*, 347–360.
(2) Abuchowski, A.; Van Es, T.; Palczuk, N. C.; Davis, F. F. *J. Biol. Chem.* **1977**, *252*, 3578–81.
(3) Langer, R.; Tirrell, D. A. *Nature* **2004**, *428*, 487–492.
(4) Veronese, F. M. *Biomaterials* **2001**, *22*, 405–417.
(5) Zalipsky, S. *Adv. Drug Delivery Rev.* **1995**, *16*, 157–82.
(6) Caliceti, P.; Veronese, F. M. *Adv. Drug Delivery Rev.* **2003**, *55*, 1261–1277.

(7) Vandermeulen, G. W. M.; Klok, H.-A. *Macromol. Biosci.* **2004**, *4*, 383–398.
(8) Donaruma, L. G. *Prog. Polym. Sci.* **1975**, *4*, 1–25.
(9) Harris, J. M.; Chess, R. B. *Nat. Rev. Drug Discov.* **2003**, *2*, 214–221.
(10) Di San Filippo, P. A.; Benedetta Fadda, M.; Rescigno, A.; Rinaldi, A.; Di Teulada, E. S. *Eur. Polym. J.* **1990**, *26*, 545–7.
(11) Bailon, P.; Berthold, W. *Pharm. Sci. Technol. Today* **1998**, *1*, 352–356.
(12) Forzani, E. S.; Zhang, H.; Nagahara, L. A.; Amlani, I.; Tsui, R.; Tao, N. *Nano Lett.* **2004**, *4*, 1785–1788.
(13) Hoffman, A. S.; Stayton, P. S. *Macromol. Symp.* **2004**, *207*, 139–151.
(14) Tu, R. S.; Tirrell, M. *Adv. Drug Delivery Rev.* **2004**, *56*, 1537–1563.
(15) Ding, Z.; Fong, R. B.; Long, C. J.; Stayton, P. S.; Hoffman, A. S. *Nature* **2001**, *411*, 59–62.
(16) Goodsell, D. S., *Bionanotechnology: Lessons from Nature*. Wiley-Loss: Hoboken, NJ, 2004.
(17) *Nanobiotechnology: Concepts, Applications and Perspectives*; Niemeyer, C. M., Mirkin, C. A., Eds.; Wiley-VCH; New York, 2004; p 469.
(18) Barron, A.; Zuckerman, R. *Curr. Opin. Chem. Biol.* **1999**, *3*, 681–687.
(19) Braunecker, W. A.; Matyjaszewski, K. *Prog. Polym. Sci.* **2007**, *32*, 93–146.
(20) Le Droumaguet, B.; Nicolas, J. *Polym. Chem.* **2010**, *1*, 563–598.
(21) Lecolley, F.; Tao, L.; Mantovani, G.; Durkin, I.; Lautru, S.; Haddleton, D. M. *Chem. Commun.* **2004**, 2026–2027.
(22) Li, H.; Bapat, A. P.; Li, M.; Sumerlin, B. S. *Polym. Chem.* **2011**, *2*, 323–327.
(23) Tao, L.; Mantovani, G.; Lecolley, F.; Haddleton, D. M. *J. Am. Chem. Soc.* **2004**, *126*, 13220–13221.
(24) Mantovani, G.; Lecolley, F.; Tao, L.; Haddleton, D. M.; Clerx, J.; Cornelissen, J. J. L. M.; Velonia, K. *J. Am. Chem. Soc.* **2005**, *127*, 2966–2973.
(25) Li, M.; De, P.; Li, H.; Sumerlin, B. S. *Polym. Chem.* **2010**, *1*, 854–859.
(26) Bontempo, D.; Heredia, K. L.; Fish, B. A.; Maynard, H. D. *J. Am. Chem. Soc.* **2004**, *126*, 15372–15373.
(27) Heredia, K. L.; Maynard, H. D. *Org. Biomol. Chem.* **2007**, *5*, 45–53.
(28) Nicolas, J.; Mantovani, G.; Haddleton, D. M. *Macromol. Rapid Commun.* **2007**, *28*, 1083–1111.
(29) Bontempo, D.; Li, R. C.; Ly, T.; Brubaker, C. E.; Maynard, H. D. *Chem. Commun.* **2005**, 4702–4704.
(30) Qi, K.; Ma, Q.; Remsen, E. E.; Clark, C. G., Jr.; Wooley, K. L. *J. Am. Chem. Soc.* **2004**, *126*, 6599–6607.
(31) Bontempo, D.; Maynard, H. D. *J. Am. Chem. Soc.* **2005**, *127*, 6508–6509.
(32) Ladmiral, V.; Mantovani, G.; Clarkson, G. J.; Cauet, S.; Irwin, J. L.; Haddleton, D. M. *J. Am. Chem. Soc.* **2006**, *128*, 4823–4830.
(33) Boerakker, M. J.; Botterhuis, N. E.; Bomans, P. H. H.; Frederik, P. M.; Meijer, E. M.; Nolte, R. J. M.; Sommerdijk, N. A. J. M. *Chem.—Eur. J.* **2006**, *12*, 6071–6080.
(34) Wilchek, M.; Bayer, E. A. *Anal. Biochem.* **1988**, *171*, 1–32.
(35) Weber, P. C.; Ohlendorf, D. H.; Wendoloski, J. J.; Salemme, F. R. *Science* **1989**, *243*, 85–8.
(36) Ueda, E. K. M.; Gout, P. W.; Morganti, L. *J. Chromatogr. A* **2003**, *988*, 1–23.
(37) Hilbrig, F.; Stocker, G.; Schläppi, J. M.; Kocher, H.; Freitag, R. *Food Bioprod. Process* **2006**, *84*, 28–36.
(38) Carter, S.; Rimmer, S.; Rutkaite, R.; Swanson, L.; Fairclough, J. P. A.; Sturdy, A.; Webb, M. *Biomacromolecules* **2006**, *7*, 1124–1130.
(39) Mattiasson, B.; Kumar, A.; Ivanov, A. E.; Galaev, I. Y. *Nat. Protoc.* **2007**, *2*, 213–220.
(40) Hart, C.; Schulenberg, B.; Diwu, Z.; Leung, W.-Y.; Patton, W. F. *Electrophoresis* **2003**, *24*, 599–610.
(41) Sigal, G. B.; Bamdad, C.; Barberis, A.; Strominger, J.; Whitesides, G. M. *Anal. Chem.* **1996**, *68*, 490–7.
(42) Gershon, P. D.; Khilko, S. *J. Immunol. Methods* **1995**, *183*, 65–76.
(43) Schmid, E. L.; Keller, T. A.; Dienes, Z.; Vogel, H. *Anal. Chem.* **1997**, *69*, 1979–1985.
(44) Xu, C.; Xu, K.; Gu, H.; Zhong, X.; Guo, Z.; Zheng, R.; Zhang, X.; Xu, B. *J. Am .Chem. Soc.* **2004**, *126*, 3392–3393.
(45) Schmitt, L.; Ludwig, M.; Gaub, H. E.; Tampe, R. *Biophys. J.* **2000**, *78*, 3275–3285.
(46) Schmitt, L.; Dietrich, C.; Tampe, R. *J. Am. Chem. Soc.* **1994**, *116*, 8485–91.
(47) Dietrich, C.; Schmitt, L.; Tampe, R. *Proc. Natl. Acad. Sci. U.S.A.* **1995**, *92*, 9014–18.
(48) Dorn, I. T.; Eschrich, R.; Seemuller, E.; Guckenberger, R.; Tampe, R. *J. Mol. Biol.* **1999**, *288*, 1027–1036.
(49) Griffith, B. R.; Allen, B. L.; Rapraeger, A. C.; Kiessling, L. L. *J. Am. Chem. Soc.* **2004**, *126*, 1608–1609.
(50) Yu, T.; Wang, Q.; Johnson, D. S.; Wang, M. D.; Ober, C. K. *Adv. Funct. Mater.* **2005**, *15*, 1303–1309.
(51) Wang, C.; Stewart, R. J.; Kopecek, J. *Nature* **1999**, *397*, 417–420.
(52) Loos, K.; Boeker, A.; Zettl, H.; Zhang, M.; Krausch, G.; Mueller, A. H. E. *Macromolecules* **2005**, *38*, 873–879.
(53) Luk, Y.-Y.; Tingey, M. L.; Hall, D. J.; Israel, B. A.; Murphy, C. J.; Bertics, P. J.; Abbott, N. L. *Langmuir* **2003**, *19*, 1671–1680.
(54) Kim, S.-Y.; Ayyadurai, N.; Heo, M.-A.; Sunghoon Park, Y. J.; Jeong, S.-G. L. *J. Microbiol. Biotechnol.* **2009**, *19*, 72–77.
(55) Rettig, H.; Krause, E.; Börner, H. G. *Macromol. Rapid Commun.* **2004**, *25*, 1251–1256.
(56) Ayres, L.; Adams, P. H. H. M.; Löwik, D. W. P. M.; van Hest, J. C. M. *Biomacromolecules* **2005**, *6*, 825–831.
(57) Matyjaszewski, K.; Xia, J. *Chem. Rev.* **2001**, *101*, 2921–2990.
(58) Teodorescu, M.; Matyjaszewski, K. *Macromolecules* **1999**, *32*, 4826–4831.
(59) Limer, A.; Haddleton, D. M. *Macromolecules* **2006**, *39*, 1353–1358.
(60) Shipp, D. A.; Wang, J.-L.; Matyjaszewski, K. *Macromolecules* **1998**, *31*, 8005–8008.
(61) Matyjaszewski, K.; Paik, H.; Zhou, P.; Diamanti, S. J. *Macromolecules* **2001**, *34*, 5125–5131.
(62) Malz, H.; Komber, H.; Voigt, D.; Hopfe, I.; Pionteck, J. *Macromol. Chem. Phys.* **1999**, *200*, 642–651.
(63) Park, S.; Cho, D.; Ryu, J.; Kwon, K.; Chang, T.; Park, J. *J. Chromatogr. A* **2002**, *958*, 183–189.
(64) Liu, S.; Pan, Q.; Xie, J.; Jiang, M. *Polymer* **2000**, *41*, 6919–6929.
(65) Gohy, J.-F.; Jerome, R.; Van den Bossche, G.; Sobry, R. *Macromol. Chem. Phys.* **1998**, *199*, 2205–2210.
(66) Zhang, L.; Eisenberg, A. *Macromol. Symp.* **1997**, *113*, 221–232.